Electronic Supplementary Material (ESI) for Materials Advances.
This journal is © The Royal Society of Chemistry 2021

Electronic Supplementary Information (ESI)

9-Fluorenyl Substitution Strategy for Aromatic-Imide-Based TADF Emitters towards Efficient and Stable Sky Blue OLED with Nearly 30% External Quantum E□ciency

Quanyou Feng,[a] Xiaojun Zheng,[a] Hongjian Wang,[a] He Zhang,[a] Yue Qian,[a] Kesheng Tan,[a] Hongtao Cao,*[a] Linghai Xie,*[a] Wei Huang[ab]

[a]*Key Laboratory for Organic Electronics and Information Displays, Institute of Advanced Materials, Nanjing University of Posts & Telecommunications, 9 Wenyuan Road, Nanjing 210023, China.* [b]*Frontiers Science Center for Flexible Electronics, Xi'an Institute of Flexible Electronics (IFE) and Xi'an Institute of Biomedical Materials & Engineering, Northwestern Polytechnical University, 127 West Youyi Road, Xi'an 710072, China.*

E-mail: iamhtcao@njupt.edu.cn, iamlhxie@njupt.edu.cn.

Contents

1. General information

The chemicals and solvents, unless otherwise specified, were purchased from Energy Chemical (Shanghai, China) or J&K Chemical Company (Beijing, China) without further purification. Toluene was dried over sodium benzophenone ketyl anion radical and distilled under a dry nitrogen atmosphere immediately prior to use. Other solvents were distilled under a dry nitrogen atmosphere immediately prior to use. The 9-phenyl-9H-fluoren-9-ol (PFOH) was synthesized according to our previous work.[1]

The ^{1}H and ^{13}C NMR spectra were recorded on Bruker® AVIII 400 MHz NMR spectrometers. GC-Mass spectra were recorded on a Shimadzu GC-MS 2010 PLUS. High-resolution mass spectra (HRMS) was obtained in positive ion atmospheric pressure chemical ionization mode on Thermo Fisher Scientific LTQ FTICR-MS. MALDI-TOF mass spectra were performed on a Bruker BIFLEX III ultrahigh-resolution Fourier transform ion cyclotron resonance (FT-ICR) mass spectrometer. Elemental analyses (C, H and N) were carried out with an Elementar vario EL III elemental analyzer. High performance liquid chromatography (HPLC) analysis was conducted on a Shimadzu Prominence-I LC2030C 3D HPLC system. HPLC traces were measured using a Sunfire C18 or XBridge BEH Shield RP18 analytical column. The single-crystal data collection was performed at 298 K on a Bruker 2000 CCD area detector using graphite-monochromated Mo Kα radiation (λ = 0.71073 Å). All structures were solved by direct methods using SHELXS-2015 and refined against F2 using SHELXL-2015. UV-visible absorption spectra were measured with a Shimadzu UV-3150 spectrometer at 298 K, and emission spectra were recorded on a Shimadzu RF-530XPC luminescence spectrometer upon excitation at the absorption maxima. Phosphorescence spectra was characterized to obtain triplet energy values of the TADF materials at 77 K. Photoluminescence quantum yields (PLQY) were were determined using Hamamatsu Absolute PL Quantum Yield Spectrometer C11347. The PL transient decay curves of the films were measured using a transient spectrometer (Edinburg FLS920) with a picosecond pulsed UV-LASTER (λ = 379 nm, pulse width = 89 ps) as the excitation source. Cyclic voltammetric studies were measured by

using an CHI660C Electrochemical Workstation in a typical three-electrode. The oxidation measurements were measured using glassy carbon electrode as the working electrode, an Ag/Ag^+ (0.01 M $AgNO_3$) as the reference electrode and Pt wire as the counter electrode in dichloromethane. Thermogravimetric analyses (TGA) were conducted on a Shimadzu DTG-60H thermogravimetric analyzer under a heating rate of 10 °C min^{-1}. Differential scanning calorimetry (DSC) analyses were performed on a Shimadzu DSC-60A Instrument at a heating rate of 10 °C min^{-1}.

All calculations were carried out using the Gaussian 09 program package.[2] The geometries in the ground state were optimized via DFT calculations at the B3LYP/6-31G (d) level. TD-DFT calculations for S_1 and T_1 using the B3LYP functional were then performed according to the geometry optimization in the lowest-lying singlet and triplet states, respectively.

Devices were fabricated by vacuum deposition onto pre-coated ITO glass substrates with sheet resistance of 15 Ω/square at a pressure lower than 1×10^{-4} mbar for organic and metal deposition. Before the fabrication of devices, the ITO glass substrates were cleaned with Decon 90, rinsed in ultrapure water and ethanol, dried in an oven at 120 °C, by plasma cleaning process. The devices were fabricated by evaporating organic onto the ITO glass substrates sequentially with an evaporation rate of 0.5~2 Å s^{-1} LiF and Al were subsquently deposited as the cathode at a deposition rate of 0.1 Å s^{-1} and 5 Å s^{-1}, respectively. EL luminescence spectra and CIE color coordinates were measured with a Spectrascan PR650 photometer, and the current-voltage characteristics were measured with a computer-controlled Keithley 2400 SourceMeter under ambient atmosphere.

2. ^{1}H NMR and ^{13}C NMR spectra

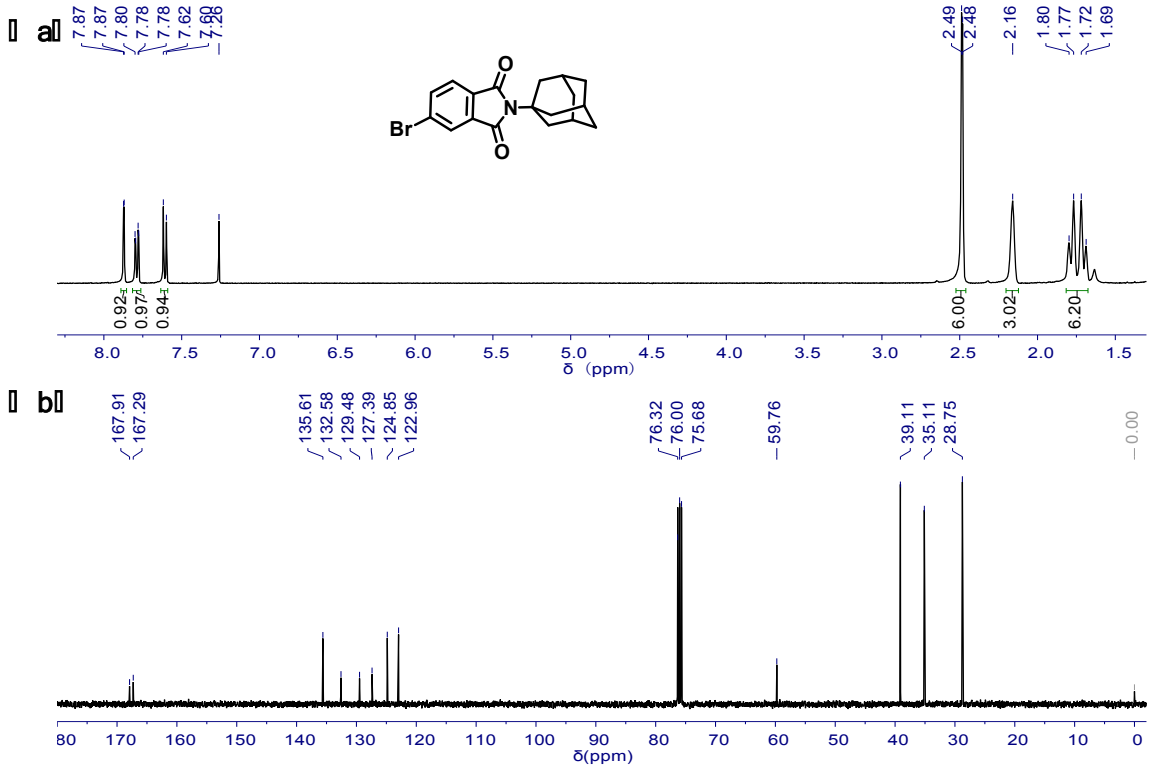

Figure S1. (a) ^{1}H NMR spectrum and (b) ^{13}C NMR spectrum of 4-BrAIAd.

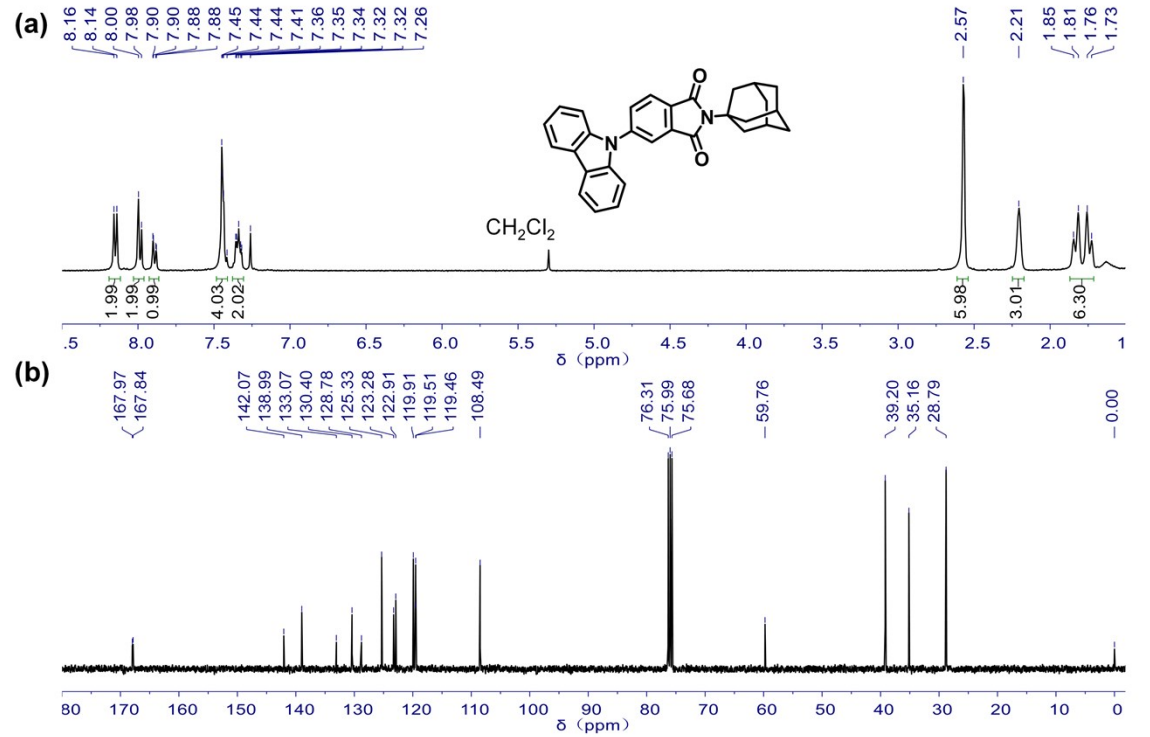

Figure S2. (a) ^{1}H NMR spectrum and (b) ^{13}C NMR spectrum of 4-CzAIAd.

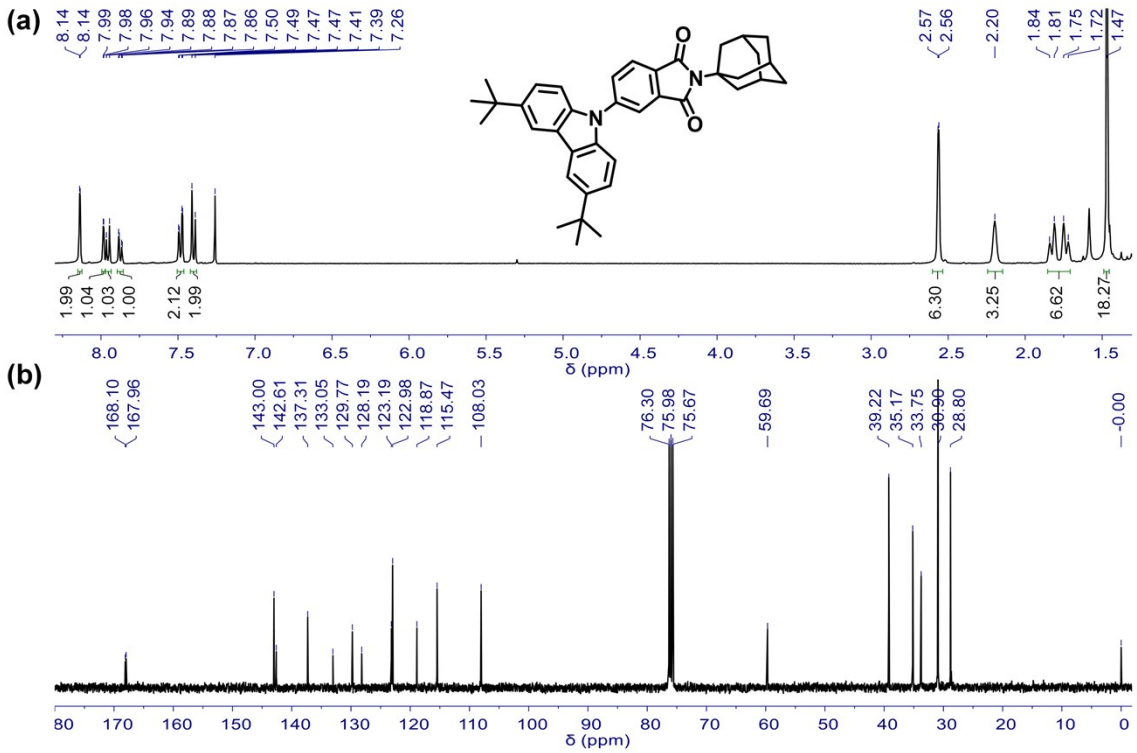

Figure S3. (a) ^{1}H NMR spectrum and (b) ^{13}C NMR spectrum of 4-TBCzAIAd.

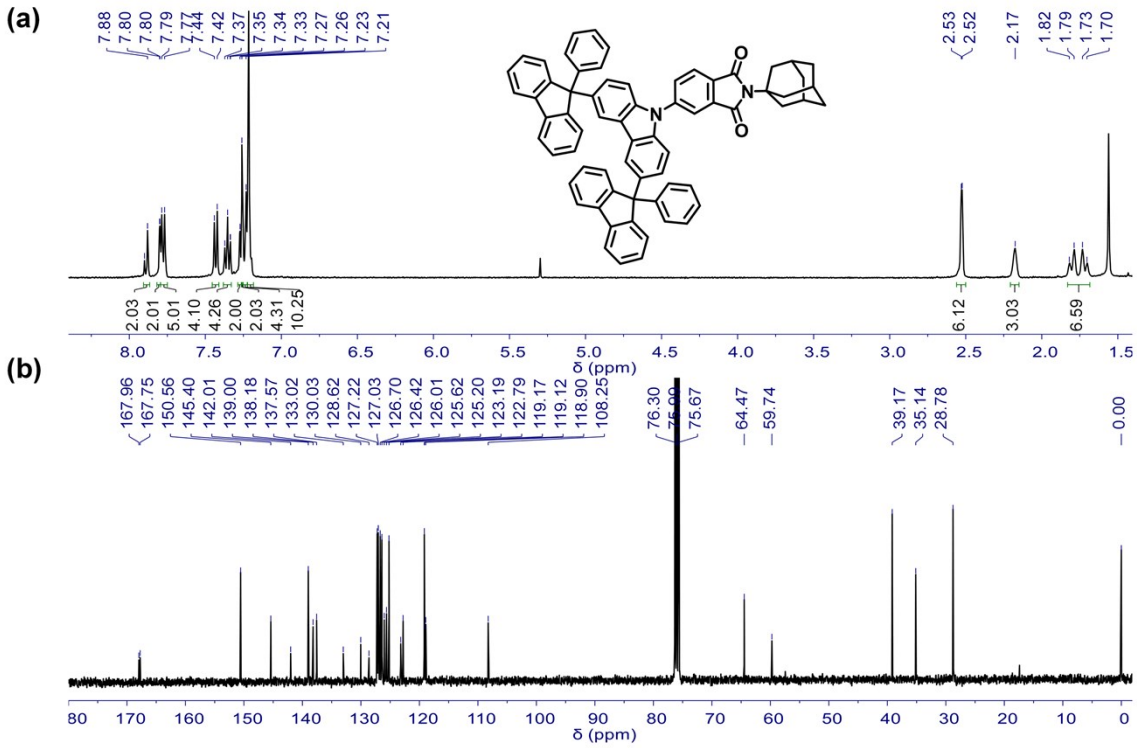

Figure S4. (a) ^{1}H NMR spectrum and (b) ^{13}C NMR spectrum of 4-DPFCzAIAd.

3. High performance liquid chromatography (HPLC) analysis

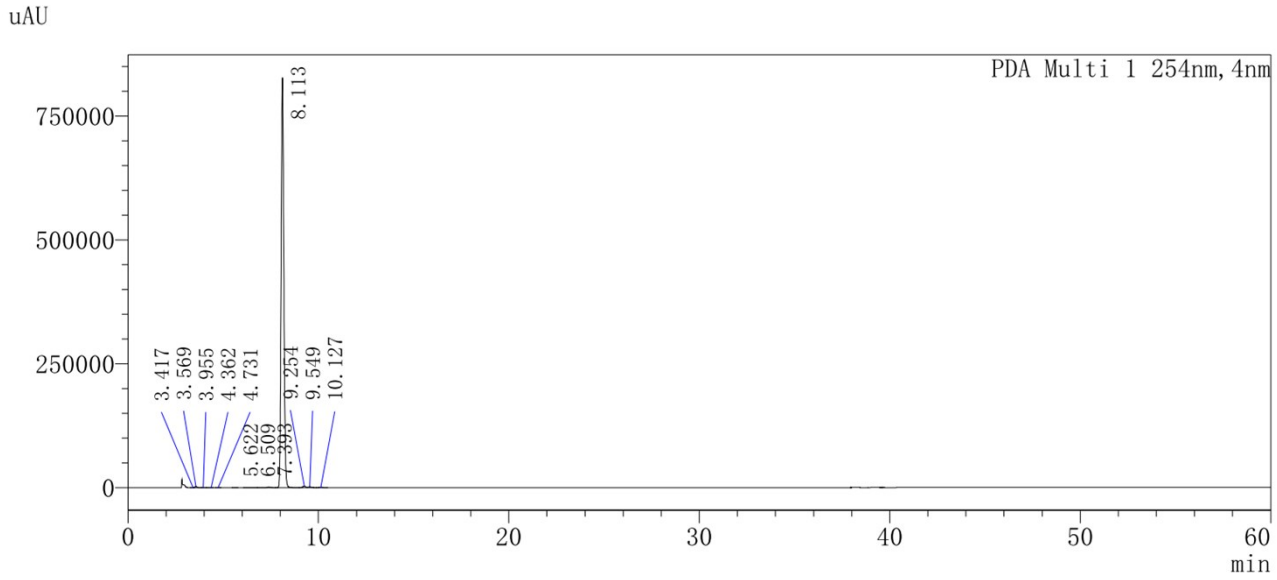

Figure S5. HPLC analysis of 4-CzAIAd.

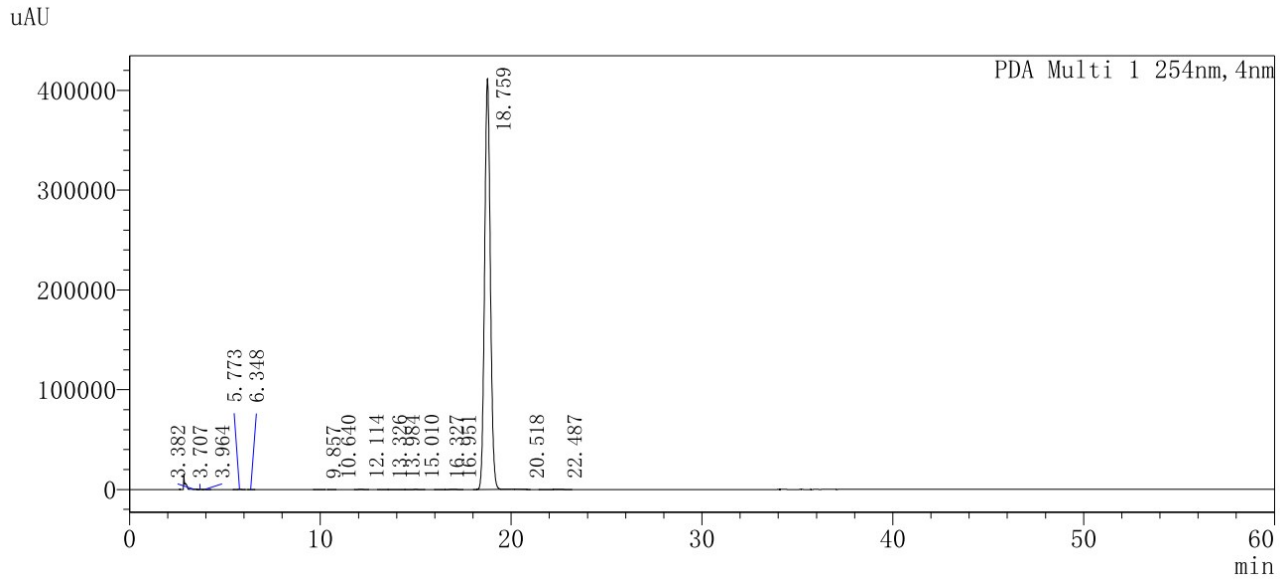

Figure S6. HPLC analysis of 4-TBCzAIAd.

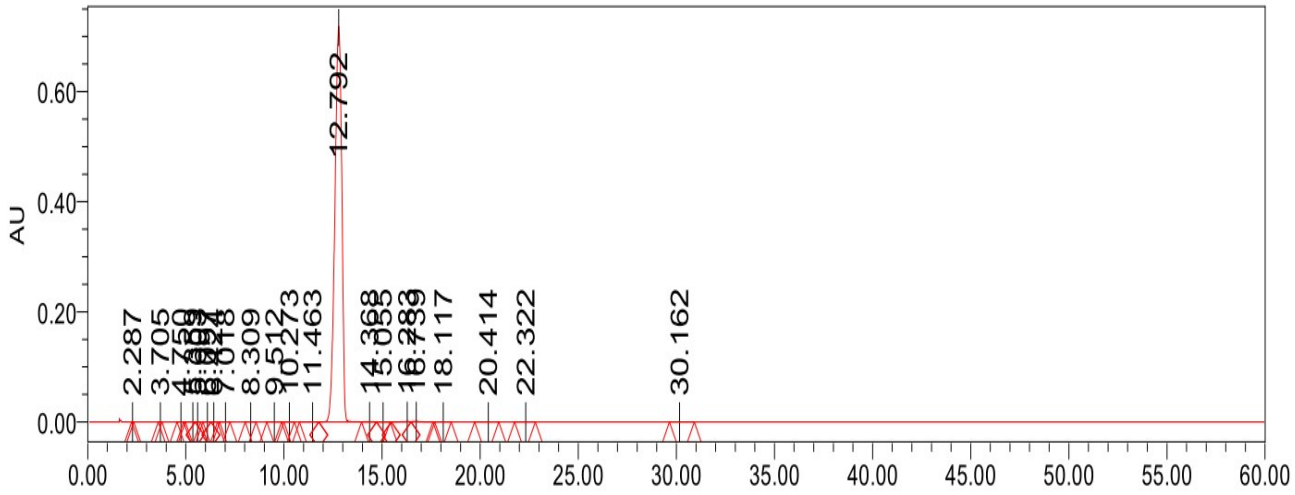

Figure S7. HPLC analysis of 4-DPFCzAIAd.

4. X-ray crystallographic data, structures and packing modes

Table S1. Crystallographic data summary.

	4-CzAIAd	4-TBCzAIAd	4-DPFCzAIAd
CCDC	2023151	2022595	2023153
Formula sum	$C_{30}H_{26}N_2O_2$	$C_{38}H_{42}N_2O_2$	$C_{68}H_{50}N_2O_2$
Formula weight	446.20 g/mol	558.32 g/mol	926.39 g/mol
Crystal system	Triclinic	Tetragonal	Triclinic
Space-group	P-1	P4 b m	P-1
Cell parameters	a=10.846Å b=13.881Å c=16.068Å, α=79.216(2)° β=73.227(2)° γ=79.654(3)°	a=11.395Å b=6.368Å c=20.823Å, α=90° β=97.252(2)° γ=90°	a=10.394Å b=14.39Å c=18.173Å, α=97.302(3)° β=98.350(3)° γ=100.019(3)°
Cell ratio	a/b=0.7814, b/c=0.8639, c/a=1.4815	a/b=1.7894, b/c=0.3058, c/a=1.8274	a/b=0.7223, b/c=0.7918, c/a=1.7484
Cell volume	2254.86 $Å^3$	1498.94 $Å^3$	2615.79 $Å^3$
Z	4	2	2
Calc. density	1.315 g/cm^3	1.238 g/cm^3	1.177g/cm^3
RAll	0.093	0.0462	0.0985
Pearson code	aP328	mP168	aP244
Formula type	NOP13Q15	NOP19Q21	NOP25Q34
Wyckoff sequence	i164	a84	i122

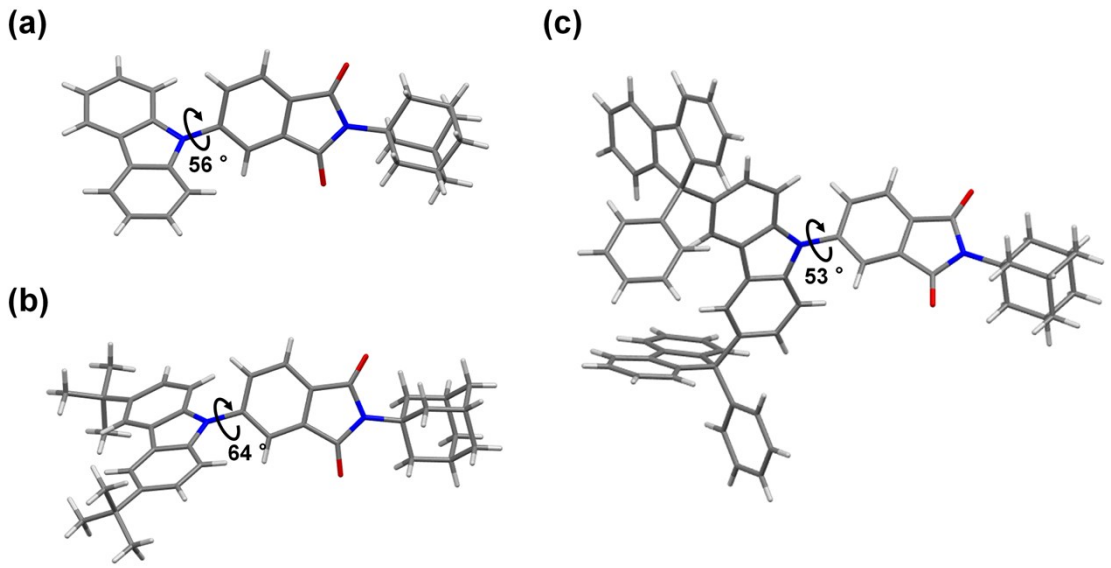

Figure S8. Single crystal structure of (a) 4-CzAIAd, (b) 4-TBCzAIAd and (c) 4-DPFCzAIAd.

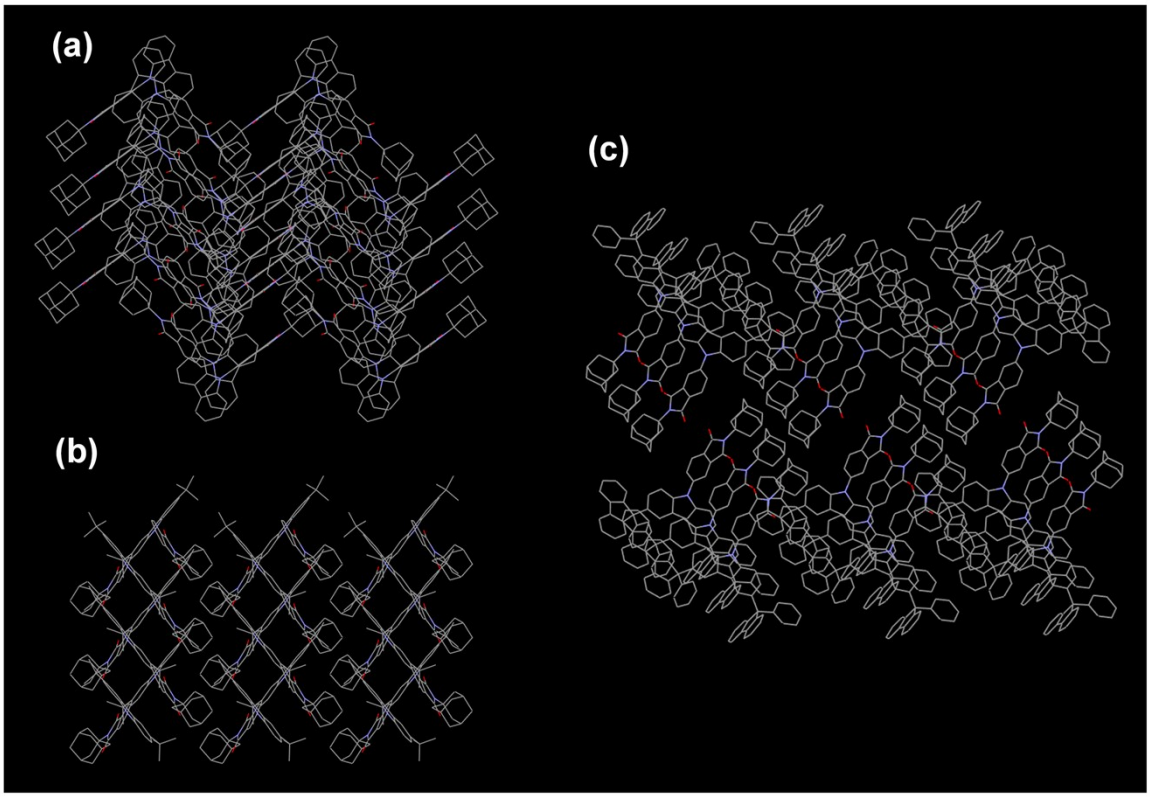

Figure S9. Packing modes of crystal structure of (a) 4-CzAIAd, (b) 4-TBCzAIAd and (c) 4-DPFCzAIAd, hydrogen atoms were omitted for clarity.

5. Photophysical properties

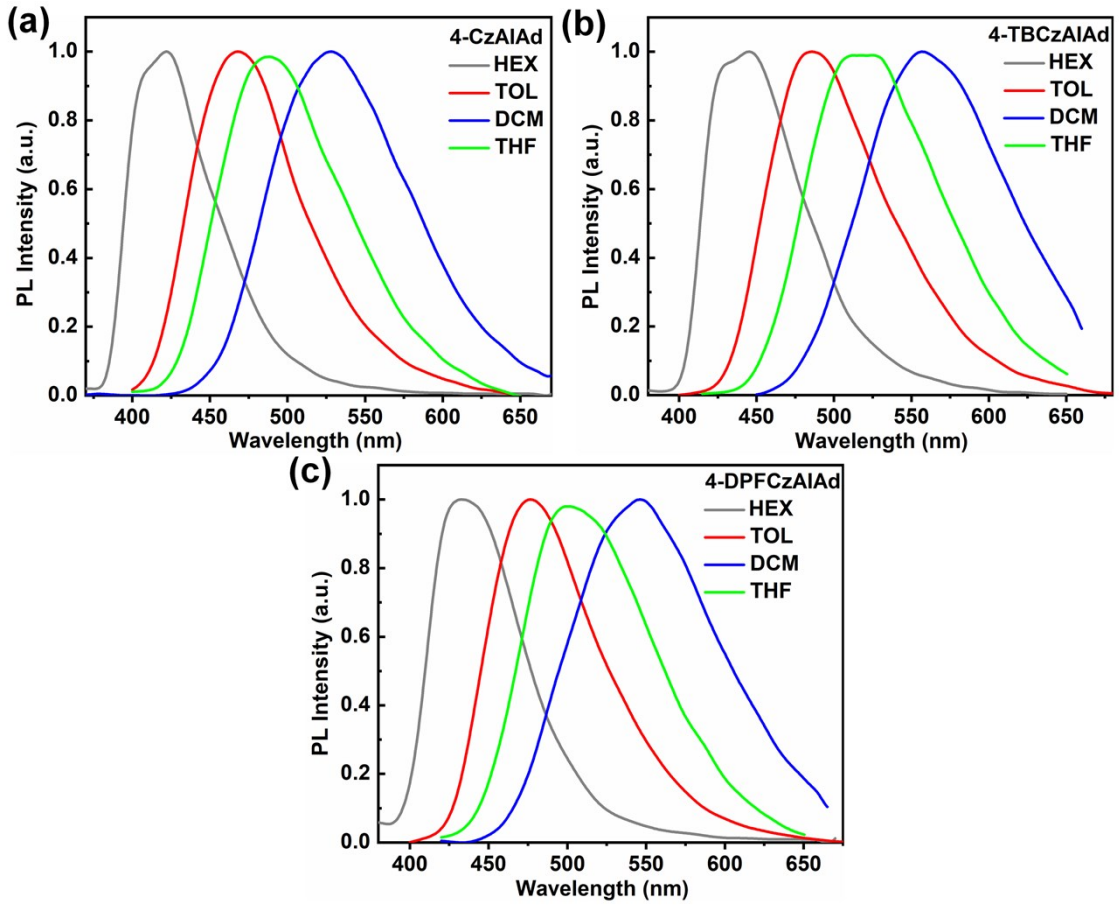

Figure S10. Emission spectra of (a) 4-CzAIAd, (b) 4-TBCzAIAd and (c) 4-DPFCzAIAd in different solvents at room temperature.

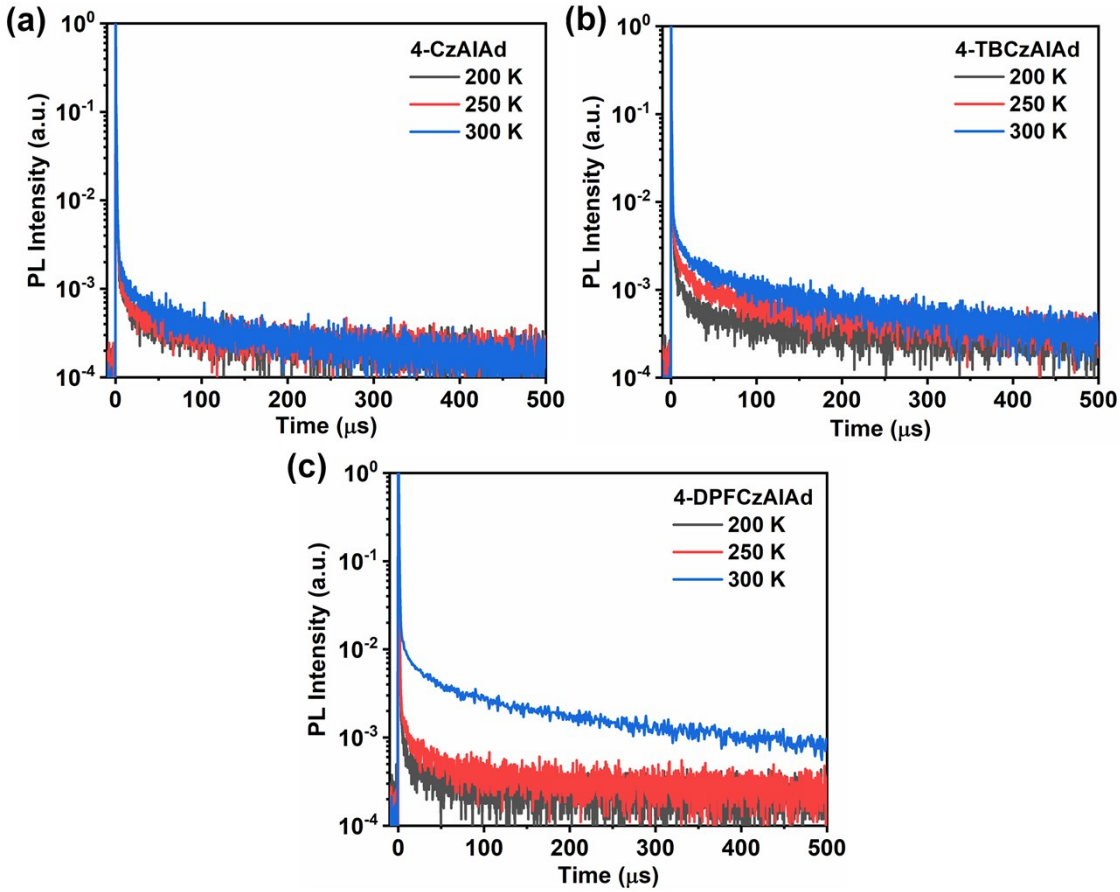

Figure S11. Temperature-dependent transient PL characteristics of (a) 4-CzAIAd, (b) 4-TBCzAIAd and (c) 4-DPFCzAIAd in 30 wt% doped DPEPO films.

6. TGA and DSC

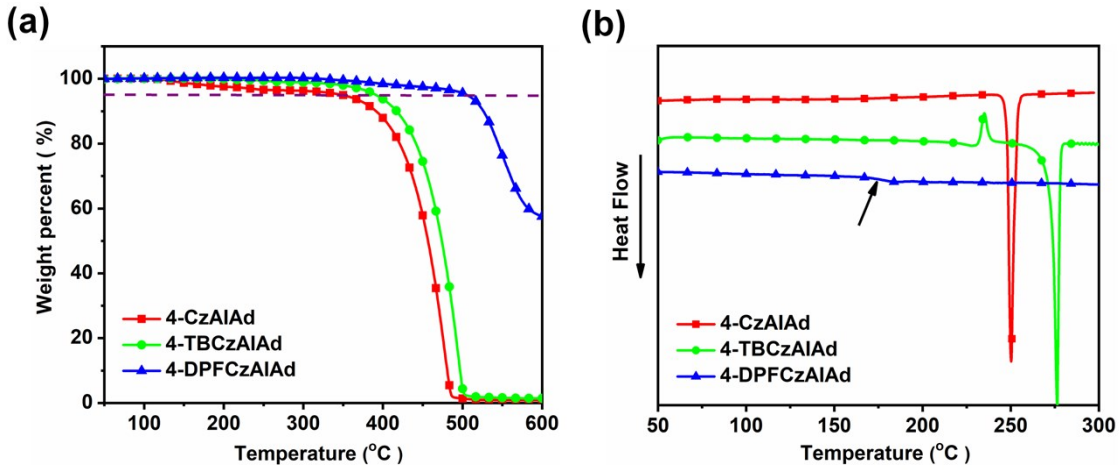

Figure S12. (a) TGA traces and (b) DSC traces of 4-CzAIAd, 4-TBCzAIAd and 4-DPFCzAIAd.

7. Device characterizations

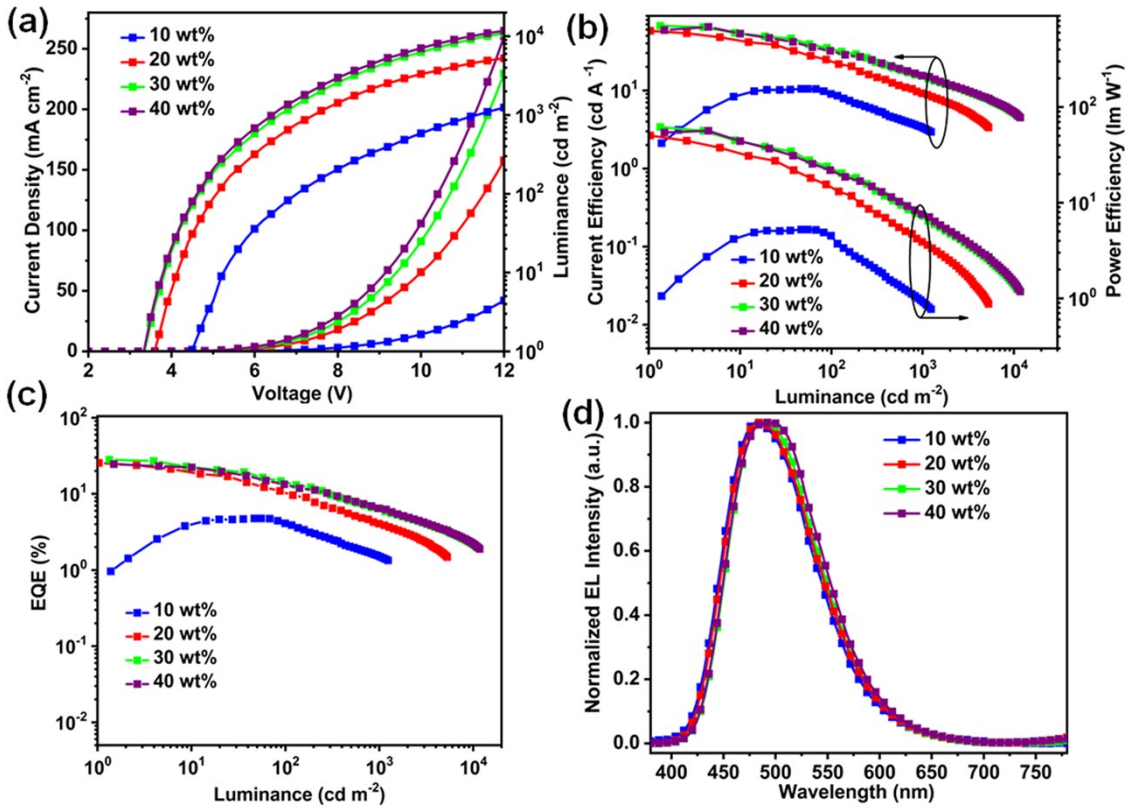

Figure S13 (a) Current density-voltage-luminance, (b) Current efficiency-luminance-power efficiency, (c) EQE-luminance characteristics and (d) EL spectra at 10 V of the OLEDs based on 4-DPFCzAIAd with different doping concentrations.

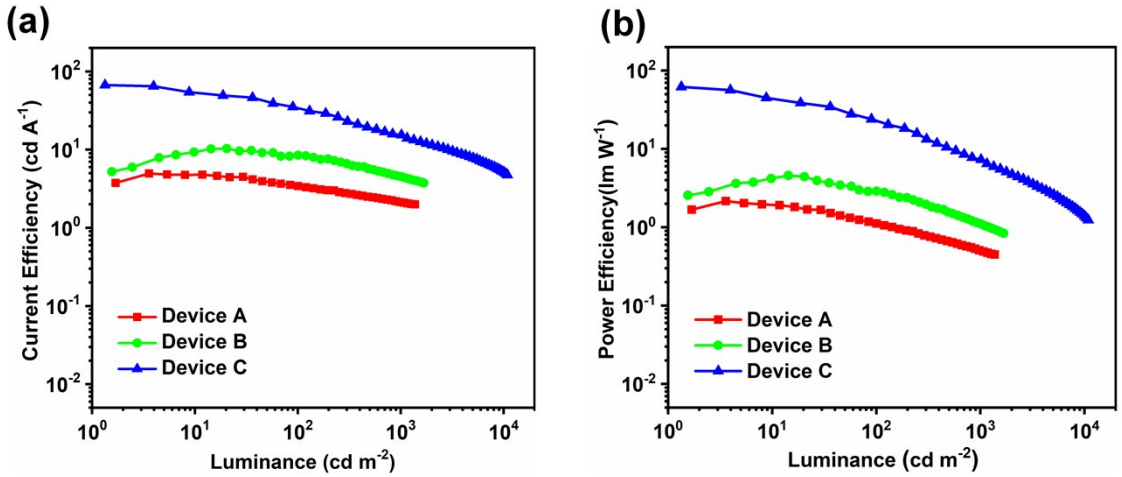

Figure S14. (a) Current efficiency-luminance, (b) power efficiency-luminance of the devices A-C.

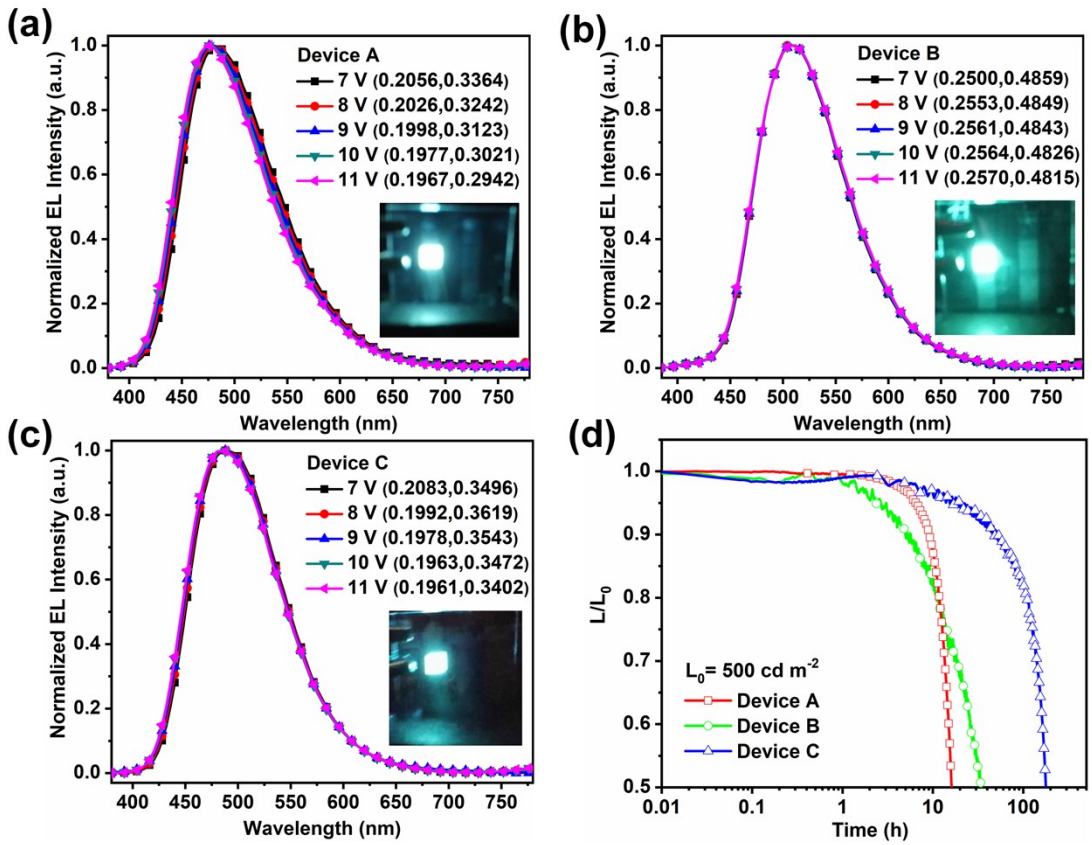

Figure S15. (a), (b), (c) EL spectra operated at different voltages of the devices (Inset: images of the emitting devices at 10 V) and (d) Lifetimes of the devices based on the three emitters.

Table S2. EL performances of 4-DPFCzAIAd based devices with different doping concentration.

Doping concentration	V_{on}[a)] [V]	λ_{EL}[b)] [nm]	CIE (x,y)	CE[c)] [cd A^{-1}]	PE[c)] [lm W^{-1}]	EQE[c)] [%]
10 wt%	4.5	482	(0.20, 0.32)	10.5/9.1/3.3/-	5.2/4.5/0.9/-	4.8/4.1/1.5/-
20 wt%	3.6	486	(0.20, 0.35)	57.7/23.8/9.2/-	50.4/14.5/3.8/-	25.5/10.4/3.9/-
30 wt%	3.4	488	(0.20, 0.36)	67.1/34.1/15.5/5.1	62.0/23.1/7.1/1.4	28.2/14.3/6.4/2.2
40 wt%	3.4	496	(0.21, 0.38)	64.9/31.7/15.5/5.3	54.4/21.6/7.1/1.5	24.6/13.3/6.3/2.2

[a)]Recorded at 1 cd m^{-2}; [b)]EL wavelength at a driving voltage of 10 V; [c)]Maximum current efficiency (CE), power efficiency (PE) and external quantum efficiency (EQE) at 100 cd m^{-2}, 1000 cd m^{-2} and 10000 cd m^{-2}, respectively.

8. References

[S1] L.-H. Xie, Q.-D. Ling, X.-Y. Hou, W. Huang, *J. Am. Chem. Soc.* **2008**, *130*, 2120.

[S2] Gaussian 09, Revision D.01, M. J. Frisch, G. W. Trucks, H. B. Schlegel, G. E. Scuseria, M. A. Robb, J. R. Cheeseman, G. Scalmani, V. Barone, B. Mennucci, G. A. Petersson, H. Nakatsuji, M. Caricato, X. Li, H. P. Hratchian, A. F. Izmaylov, J. Bloino, G. Zheng, J. L. Sonnenberg, M. Hada, M. Ehara, K. Toyota, R. Fukuda, J. Hasegawa, M. Ishida, T. Nakajima, Y. Honda, O. Kitao, H. Nakai, T. Vreven, J. A. Montgomery, Jr., J. E. Peralta, F. Ogliaro, M. Bearpark, J. J. Heyd, E. Brothers, K. N. Kudin, V. N. Staroverov, T. Keith, R. Kobayashi, J. Normand, K. Raghavachari, A. Rendell, J. C. Burant, S. S. Iyengar, J. Tomasi, M. Cossi, N. Rega, J. M. Millam, M. Klene, J. E. Knox, J. B. Cross, V. Bakken, C. Adamo, J. Jaramillo, R. Gomperts, R. E. Stratmann, O. Yazyev, A. J. Austin, R. Cammi, C. Pomelli, J. W. Ochterski, R. L. Martin, K. Morokuma, V. G. Zakrzewski, G. A. Voth, P. Salvador, J. J. Dannenberg, S. Dapprich, A. D. Daniels, O. Farkas, J. B. Foresman, J. V. Ortiz, J. Cioslowski, and D. J. Fox, Gaussian, Inc., Wallingford CT, **2013**.